

## Density functional theory study of hexagonal carbon phases

This article has been downloaded from IOPscience. Please scroll down to see the full text article.

2009 J. Phys.: Condens. Matter 21 235401

(<http://iopscience.iop.org/0953-8984/21/23/235401>)

View [the table of contents for this issue](#), or go to the [journal homepage](#) for more

Download details:

IP Address: 129.252.86.83

The article was downloaded on 29/05/2010 at 20:07

Please note that [terms and conditions apply](#).

# Density functional theory study of hexagonal carbon phases

Zhibin Wang, Faming Gao<sup>1</sup>, Na Li, Nianrui Qu, Huiyang Gou and Xianfeng Hao

Department of Applied Chemistry, Yanshan University, Qinhuangdao 066004, People's Republic of China

E-mail: [fmgao@ysu.edu.cn](mailto:fmgao@ysu.edu.cn)

Received 28 November 2008, in final form 3 April 2009

Published 11 May 2009

Online at [stacks.iop.org/JPhysCM/21/235401](http://stacks.iop.org/JPhysCM/21/235401)

## Abstract

It is reported frequently that the new carbon phases may be harder than diamond (Wang *et al* 2004 *Proc. Natl Acad. Sci.* **101** 13699 and Mao *et al* 2003 *Science* **302** 425). However, the mechanism is still unclear. In this paper we systematically investigate the structural, electronic, and mechanical properties of the diamond polytypes using first-principles density functional calculations. The results show that the bulk modulus and shear modulus for the hexagonal form of diamond approach those of diamond, suggesting they might be hard and low compressibility materials. According to the semiempirical method for hardness based on the Mulliken overlap population, the hardnesses for hexagonal forms have been evaluated and compared to diamond. The results indicate that these phases are superhard. More importantly, the bonds in some specific directions of the hexagonal phases are harder than those in diamond, which may lead to the noticeable indentation marks on the diamond anvils observed in experiments.

(Some figures in this article are in colour only in the electronic version)

## 1. Introduction

Due to the promising industrial applications of superhard materials, widespread attention has been devoted to designing new low compressibility materials [1–3]. It has long been known that the element carbon can exist in various forms, such as graphite (soft phase), fullerenes, nanotubes, cubic diamond (the hardest phase as known at present), nH diamond, etc [4], owing to its flexibility of bond hybridization. Researchers always expect to find a new carbon phase with hardness reaching or even exceeding that of diamond via high-pressure phase transformation, laser-induced reactive quenching processing, or x-ray induced synthesis of graphite or other carbon polytypes [5–13]. Recently, graphite was squeezed at room temperature and a new phase was observed at a pressure of ~17 GPa which left a ring crack indentation on the diamond anvils [9]. However, experiment revealed this new structure was quenchable only at low temperatures ( $T < 100$  K) [6–9]. Furthermore, Wang *et al* [14] found that when the carbon nanotubes were cold compressed to over 100 GPa in the diamond anvil cell, the obtained new high-

pressure hexagonal form (2H diamond) could be preserved at ambient conditions, which made a noticeable indentation mark on the diamond anvils. These experimental results thus indicate that the new forms of carbon may be as hard as or harder than diamond, and this avenue might be one of the potential strategies employed for the development of superhard and ultraincompressibility materials. In addition, 8H diamond was produced by using an x-ray induced reactive processing at ambient pressure [15]. On the other hand, theoretical investigations of these fascinating phases of carbon are scarce, and it is still not clear if the new forms are harder than cubic diamond. More importantly, a problem of great importance that should be clarified is the origin of the noticeable indentation mark on the diamond anvils in experiments. First-principles calculation is one strong and useful tool to provide further details about the crystal structure and its corresponding mechanical properties are highly desirable. So far no systematic first-principles calculations for these four phases have been reported. In addition, it is well known that the correlation between the hardness and the bulk/shear modulus ( $B/G$ ) is not unequivocal and monotonic, and then, the evaluation of hardness on the basis of the Mulliken overlap population is essential.

<sup>1</sup> Author to whom any correspondence should be addressed.

**Table 1.** The hexagonality of diamond  $h\%$ , calculated equilibrium lattice parameters  $a_0$  (Å),  $c_0$  (Å), density  $\rho$  (g cm<sup>-3</sup>), zero-pressure elastic constants  $c_{ij}$  (GPa), bulk modulus  $B$  (GPa), shear modulus  $G_h$  (GPa), compression anisotropy factor  $A_{\text{comp}}$ , the shear elastic anisotropy factor  $A_{\text{shear}}$ , and the equilibrium energy  $E_o$  (eV/atom).

	2H			4H			8H			C diamond	
	GGA	LDA	Expt.	GGA	LDA	Expt.	GGA	LDA	Expt.	GGA	LDA
$h\%$	100			50			25			0	
$a_0$	2.486	2.480	2.496 <sup>a</sup> 2.52 <sup>b</sup>	2.492 77	2.487 17	2.522 <sup>d</sup>	2.496 85	2.491 27	2.481(6) <sup>e</sup>	2.500	2.495
$c_0$	4.139	4.139(9)	4.123 <sup>a</sup> 4.12 <sup>b</sup>	8.222 99	8.205 78	8.234 <sup>d</sup>	16.393	16.357 2	16.268(60) <sup>e</sup>	6.123 75 <sup>f</sup>	6.111 503 <sup>f</sup>
$\rho$	3.59	3.62	3.6 ± 0.2 <sup>a</sup>	3.605 75	3.629 6		3.605 58	3.629 7	3.67 <sup>e</sup>		
$c_{11}$	1235	1250		1210	1229		1198	1217		1093	1093
$c_{33}$	1337	1375		1289	1309		1250	1274			
$c_{44}$	483	475		491	504		510	504		589	593
$c_{12}$	86	99		94	94		87	98		118	135
$c_{13}$	4	6		26	27		39	41			
$c_{66}$	575	576		558	568		555	559			
$B$	444	455	447 <sup>a</sup> 462 <sup>c</sup>	445	451		442.4	452.5	460–462 <sup>e</sup>	443	454
$G_h$	552	551		543	554		546	547			
$A_{\text{comp}}$	0.9848	0.9768		0.991 6	0.989 7		0.996 6	0.999 9			
$A_{\text{shear}}$	0.8416	0.8260		0.879 8	0.886 9		0.918 9	0.901 3			
$-E_o$	156	155.5		156.01	155.53		156.01	155.54		156	155.5

<sup>a</sup> Reference [11]; <sup>b</sup> Reference [32]; <sup>c</sup> Reference [13]; <sup>d</sup> Reference [22]; <sup>e</sup> Reference [15].

<sup>f</sup> Reference [23]. In the cubic diamond, the lattice constant  $c$  is determined by the ideal ratio  $c/(3a) = 0.8165$ .

In this paper, the first-principles calculations technique was employed to study their electronic properties, mechanical properties as well as their stabilities relative to the parent cubic structure. Particularly, according to the estimation of the hardness for the specific bond, we elucidate why a noticeable indentation mark on the diamond anvils was made by the hexagonal diamond phase (2H diamond).

## 2. Calculating details

The structure of the hexagonal diamond proposed by Wang *et al* was used as input for the calculations. Its unit cell contains four carbon atoms [14]. The internal coordinates for the four carbon atoms in the unit cell are  $\pm(1/3 \ 2/3 \ z, 2/3 \ 1/3 \ 1/2 + z)$  with  $z = 1/16$  derived from lonsdaleite. The 4H and 8H diamond were investigated computationally. Furthermore, the cubic diamond (C diamond) has been calculated for comparison. The first-principles calculations are performed using the CASTEP code [16] based on the density functional theory (DFT). The electrons exchange and correlation functional were treated by the generalized gradient approximation (GGA) proposed by Perdew–Wang (PW91) [17], which was designed to be more robust and accurate than the original GGA, as well as the local density approximation (LDA) using the Ceperley–Alder expression as parameterized by Perdew and Zunger (LDA-CAPZ) [18]. The calculations were performed using the Vanderbilt ultrasoft pseudopotentials for the atom [19], which generated the atomic configuration of C as  $2s^2 2p^2$ , and an energy cutoff of 310 eV, for the plane wave basis set. The Brillouin zone  $k$ -points are generated by the Monkhorst–Pack scheme [20], that is a  $12 \times 12 \times 6$   $k$  point mesh for 2H diamond,  $8 \times 8 \times 8$  for cubic diamond,  $12 \times 12 \times 4$  for 4H diamond,  $12 \times 12 \times 2$  for 8H diamond. The coordinate optimization of the lattice is realized using the Broyden–Fletcher–Goldfarb–Shanno (BFGS) minimization algorithm by taking into account

the energy as well as the gradients to relax the atomic positions [21]. Furthermore, increasing the cutoff energy to 500 eV changes the lattice constants by less than 0.1%, which indicates that these calculations are reliable.

## 3. Results and discussions

The calculated lattice constants of the diamond polytypes described above within both GGA and LDA are shown in table 1. It can be seen that the calculated parameters  $a_0$  and  $c_0$  of unit cells both with GGA and LDA are excellently consistent with the experimental values, with an error less than 1% for 2H- and 8H-, 1.4% for 4H diamond. This indicates that the computations based on the DFT are reliable to characterize the crystal structure considered in this paper. Furthermore, the predictable equilibrium lattice parameters of cubic diamond are also listed in table 1. The results show clear trends with the hexagonality [23]. The lattice constant  $a_0$  increases, whereas the normalized lattice constant  $c_0/n$  and the ratio  $c_0/(na)$  decrease with decreasing hexagonality. This is in agreement with other calculations [23, 24]. Due to the small difference among the structure of the bonding configuration of the diamond polytypes, their properties calculated here look very similar, though they are formed by varying the bilayers stacking sequence along the hexagonal  $c$ -axis direction.

Elastic constant is a key factor to understand the mechanical behavior and physical properties of a material. For a hexagonal crystal, the five independent non-zero elastic stiffness constants  $c_{ij}$  are usually chosen to be  $c_{11}$ ,  $c_{12}$ ,  $c_{13}$ ,  $c_{33}$ , and  $c_{44}$  [25]. A sixth non-independent constant is  $c_{66} = (c_{11} - c_{12})/2$ . Hence, the whole set of zero-pressure elastic constants  $c_{ij}$  for the 2H, 4H, and 8H diamond have been calculated by the static and rapidly converging fluctuation methods [26] and tabulated in table 1. Whether the stability conditions for the hexagonal structure are fulfilled has been examined by the

well-known stability criteria listed below [27]:

$$c_{11} > 0, \quad c_{33} > 0, \quad c_{44} > 0,$$

$$c_{11} - c_{12} > 0, \quad (c_{11} + c_{12})c_{33} - 2c_{13}^2 > 0.$$

The computational results both with GGA and LDA satisfy the stability criteria suggesting all the structures discussed here are mechanically stable.

The zero-pressure bulk modulus and energy were also obtained by *ab initio* calculations. The bulk modulus of the 2H diamond within GGA (LDA), 444 GPa (455 GPa), was slightly smaller (larger) than that of the former literature data [14], 447 GPa, falling into an error of  $\sim 2\%$ , indicating a potential low compressibility material. That there is good agreement between the calculated bulk modulus of 2H, 4H, and 8H diamond with that of cubic diamond indicates that the bulk modulus is rather insensitive to the corresponding structure considered. In addition, the elastic anisotropy, which is intimately associated with the mechanical properties especially in engineering applications, is examined qualitatively below. The small  $B/G$  value (the quotient of the bulk to shear modulus),  $\sim 0.8$ , demonstrates the large brittleness of these hexagonal structures according to the Pugh criterion [28–30]. Besides, the compression anisotropy factor  $A_{\text{comp}}$  and the shear elastic anisotropy factor  $A_{\text{shear}}$  are available respectively for checking the degree of the elastic anisotropy of the hexagonal crystal structure complying with [28]. For 2H diamond [14],  $A_{\text{comp}} = 0.9848$  and  $A_{\text{shear}} = 0.8416$  (obtained within GGA) suggesting that this phase has relatively small compressive anisotropy and somewhat larger shear anisotropy among the structure discussed. As can be seen from table 1, both factor  $A_{\text{comp}}$  and factor  $A_{\text{shear}}$  show a clear trend with the varying hexagonality ( $h\%$ ), which indicate that the 8H diamond has better isotropy among these nH diamond polytypes. Moreover, it is interesting to note that total energy per carbon atom of the hexagonal phase calculated, either within GGA or LDA, approaches that of cubic diamond, as given in table 1. Therefore, it is supposed that the structures are energetically stable.

The band structure is calculated on the hexagonal lattice at the theoretical equilibrium constant. The energy bands of the phases considered here along high-symmetry lines of the Brillouin zone are presented graphically in figures 1(a)–(d). As shown in figure 1, the top of the valence bands for all the diamond polytypes discussed above is situated at the G point and the valence-band width is about 22 eV for each. But the position of the conduction-band minimum varies for the different polytype structures. Furthermore, the fundamental gap of the 2H diamond between the valence and conduction bands,  $\sim 3.6$  eV (a), is indirect occupying a space between the K and the G points of the Brillouin zone, which is the minimum among the structures discussed above, 4.81 eV for 4H (b), 4.65 eV for 8H (c), and 4.4 eV for 3C diamond (d). Due to the underestimation of the density functional method, the exact band gap of these crystals should be wider. All of the results predict semiconducting character.

To further understand electronic properties, the partial and total densities of states (DOS) of diamond polytypes

**Table 2.** Bond length of  $\mu$ -type,  $d^\mu$  (Å), Mulliken bond overlap population of  $\mu$ -type  $P^\mu$ , band volume of  $\mu$ -type  $v_b^\mu$  (Å<sup>3</sup>), calculated hardness of  $\mu$ -type bond  $H_{\text{vcalc}}^\mu$  (GPa), calculated hardness  $H_{\text{calc}}$  (GPa), and experimental hardness  $H_{\text{exp}}$  (GPa).

	Bond	$d^\mu$	$P^\mu$	$v_b^\mu$	$H_{\text{vcalc}}^\mu$	$H_{\text{calc}}$	$H_{\text{exp}}$
2H	C–C	1.5264	0.85	2.7370	117.5	55	60–70 <sup>a</sup>
	C–C	1.5507	0.43	2.8698	54.9		
4H	C–C	1.5285	0.8267	2.7488	113.4	63.2	
	C–C	1.5276	0.53	2.7439	72.9		
8H	C–C	1.5539	0.5	2.8883	63.2		
	C–C	1.5293	0.82667	2.7535	113.1	63.8	
	C–C	1.5305	0.82667	2.7598	112.7		
	C–C	1.5302	0.53	2.7579	72.3		
Diamond <sup>a</sup>	C–C	1.5354	0.52	2.7862	69.8		
	C–C	1.5509	0.5	2.8714	63.8		
	C–C	1.531	0.75	2.836	97.7	97.7	96 $\pm$ 5

<sup>a</sup> Reference [33] hardness of lonsdaleite.

described above are also calculated at zero pressure, as given in figures 1(e)–(h), where the vertical dashed lines show the Fermi level ( $E_F$ ). The DOS indicate that the low valence band is mainly from the s orbitals of C atoms and p electrons contribute more to the highest valence band, while the conduction band is from the greater contributions of the p electrons of C atoms for every polytype considered in this paper. Also, the valence electrons' distributions of these diamond phases have been given to give a sense of the bonding properties (figure 2). From figure 2, we find that strong covalency is presented. It is also shows clearly that the charge density distribution of 4H (c) and 8H (d) diamond combines features from both 3C (a) and 2H diamond (b). Together with the DOS, the  $sp^3$ -bond character of 2H, 4H, and 8H carbon, like that of 3C, is revealed by the calculated charge density distribution, which may explain the higher bulk modulus of diamond polytypes.

Due to the higher bulk modulus comparable to that of the cubic diamond and the experiment phenomena that indentation cracks on the diamond anvils made by the new 2H carbon phase, the hexagonal structure crystal was expected to be harder than cubic diamond in some limited regions [14]. In order to clarify this aspect, the hardness calculation seems to be of great interest and necessary. According to the intrinsic hardness theory based on the Mulliken overlap population [31], the intrinsic hardness of the new hexagonal carbon phase can be calculated as follows:

$$H_v^\mu (\text{GPa}) = 740P^\mu (v_b^\mu)^{-5/3},$$

where  $P^\mu$  is the Mulliken overlap population of a  $\mu$ -type bond, and  $v_b^\mu$  is the  $\mu$ -type bond volume. The calculated hardness results of diamond polytypes are given in table 2. Although the hardness of the 2H, 4H, and 8H diamond are almost equal, a clear trend for the hardness of various bonds can be seen in table 2: The largest hardnesses of bonds in the 2H, 4H, and 8H diamond are respectively 117.5, 113.4, 113.1 GPa, which decrease with the decreasing of the hexagonality; while the smallest hardnesses of bonds in the 2H, 4H, and 8H diamond are respectively 54.9, 63.2, 63.8 GPa, which increase with the decreasing of the hexagonality. Generally, the weakest

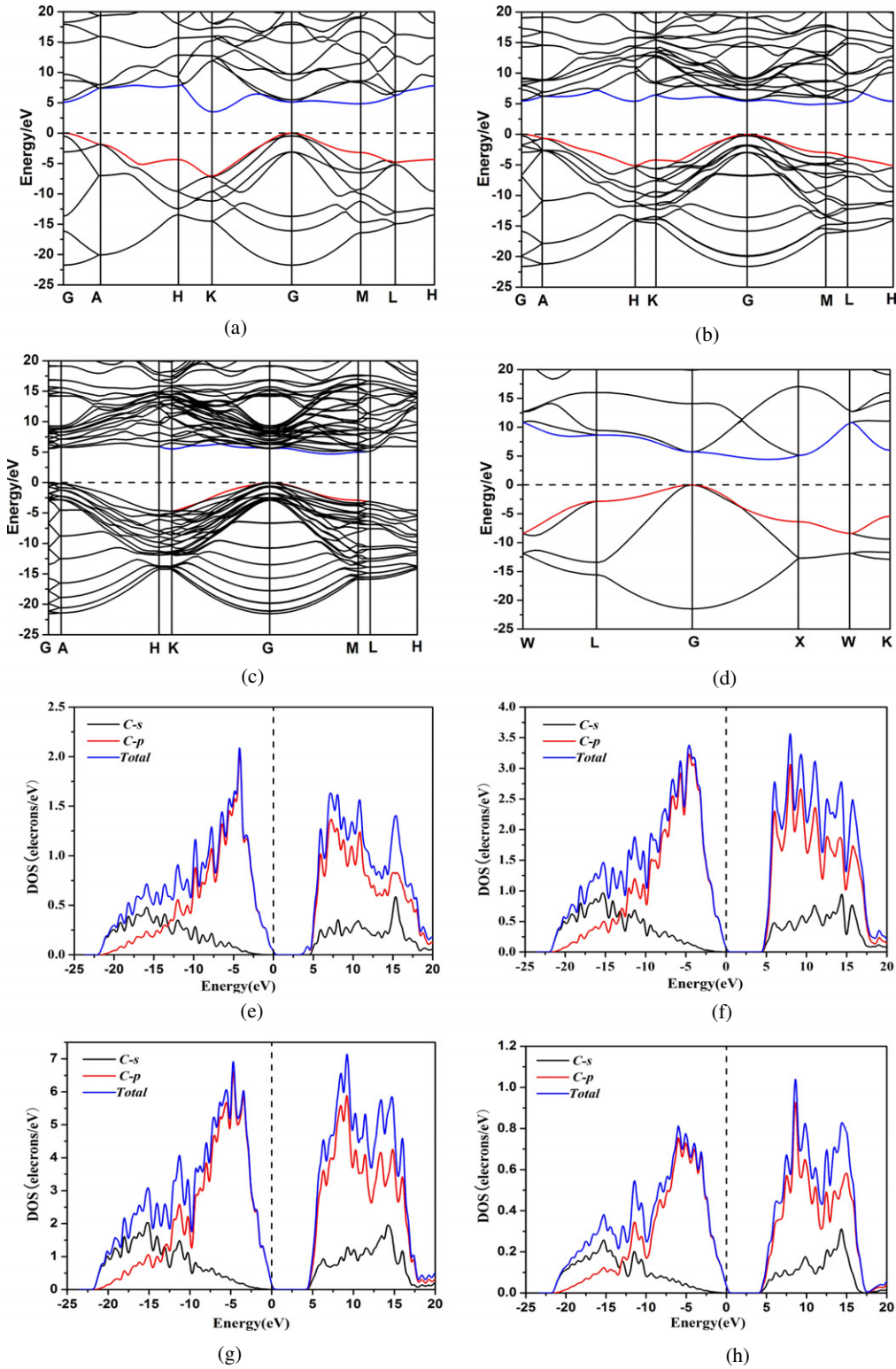


**Figure 1.** Calculated band structure of the diamond polytype, (a) is 2H diamond, (b) 4H diamond, (c) 8H diamond, and (d) cubic diamond. (e)–(h) is the partial and total density of states (DOS) of 2H, 4H, 8H, and 3C diamond, respectively. The Fermi level shifts to 0 eV.

bond determines the measurable hardness of materials. So the minimum  $H_v^\mu$  is considered as the materials' calculated hardness. Obviously, all of the structures referred to are superhard materials.

According to the bond lengths existing in the cell, all bonds in per unit cell of the 2H diamond could be classified

into two groups, with lengths of 1.5264 Å and 1.5507 Å respectively. The bond length of the cubic diamond is consistent with the former theoretical result [28]. We found that the longer bonds, 1.5507 Å, which were only along the *c*-direction, were softer than the shorter ones. According to [31], the weakest bond plays a determinative role in the hardness of

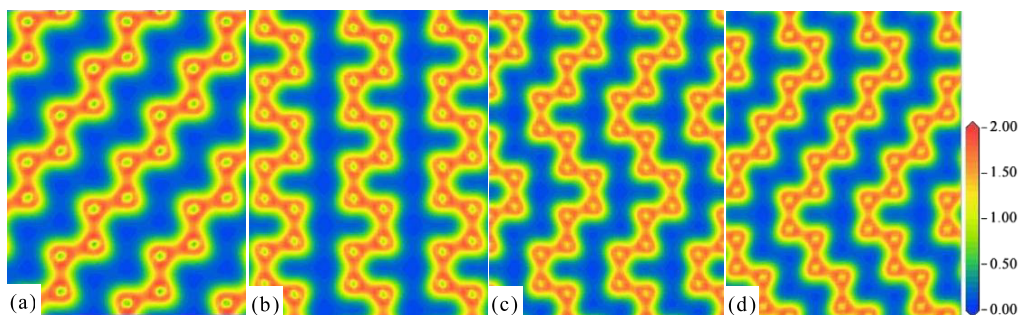


**Figure 2.** Charge density distributions of the diamond polytypes, (a) 3C diamond, (b) 2H, (c) 4H, (d) 8H. The lighter shade shows the section of a strong covalent bond.

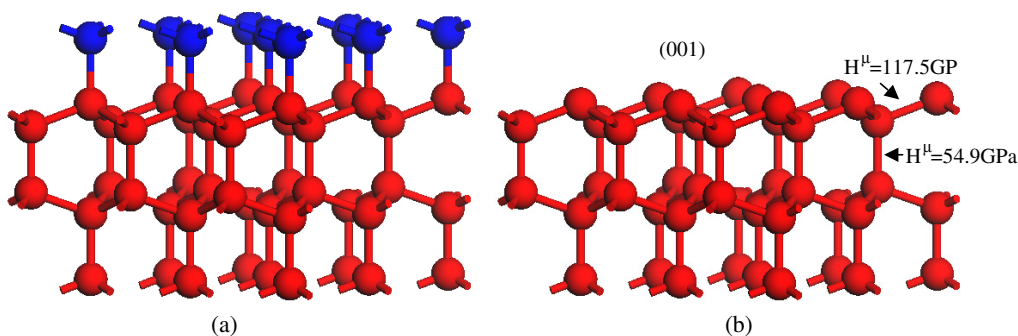


**Figure 3.** (a) Crystal structure of the 2H diamond phase, vertical on the paper is the direction of the  $c$ -axis in the crystal lattice. (b) Hardness of (001) top layer crystal structure of the 2H diamond carbon phase at 117.5 GPa.

materials. Breaking the bonds will start from softer ones when there are differences in the strength among different types of bonds. In other words, the lowest hardness of the 2H diamond phase measured macroscopically should be about 55 GPa. But in a certain direction, such as some (001) plane with shorter bonds only as shown in figure 3(b), the bond hardness (117.5 GPa) is larger than that of diamond ( $\sim 97.7$  GPa). It is possible that the indentation mark on the diamond anvils was made when the crystal grain with the surface in the (001) plane, shown in figure 3(b), contacted with the surface of the diamond anvils.

#### 4. Conclusion

In summary, the structural, elastic, and electronic properties of the 2H, 4H, and 8H diamond have been presented using first-principles calculations. The calculated results are consistent with either the available experimental results or other calculated values. The hardness calculations based on the Mulliken overlap population indicate that the  $n$ H carbon phases are superhard materials. Moreover, the ultrahard bonds in specific directions in the new hexagonal 2H phase (117.5 GPa) are harder than those of the diamond (97.7 GPa), which might be the origin of the noticeable indentation mark on the diamond anvils observed experimentally. Combined with the other excellent properties discussed, this means that  $n$ H diamonds have a promising future.

#### Acknowledgments

The authors acknowledge the financial support from the National Natural Science Foundation of China (grant No. 50672080) and the Natural Science Foundation of Hebei (grant E2008000785), and A Foundation for the Author of National Excellent Doctoral Dissertation of PR China (No. 200434).

#### References

- [1] Han S, Ihm J, Louie S G and Cohen M L 1998 *Phys. Rev. Lett.* **80** 995
- [2] Zheng J C 2005 *Phys. Rev. B* **72** 052105
- [3] Gou H Y, Hou L, Zhang J W, Li H, Sun G F and Gao F M 2006 *Appl. Phys. Lett.* **88** 221904
- [4] Phelps A W, Howard W and Smith D K 1993 *J. Mater. Res.* **8** 2835
- [5] Zhang B and Guo W L 2005 *Appl. Phys. Lett.* **87** 051907
- [6] Miller E D, Nesting D C and Badding J V 1997 *Chem. Mater.* **9** 18
- [7] Yin M T and Cohen M L 1983 *Phys. Rev. Lett.* **50** 2006
- [8] Bundy F P 1963 *J. Chem. Phys.* **38** 631
- [9] Mao W L, Mao H K, Eng P J, Trainor T P, Newville M, Kao C C, Heinz D L, Shu J F, Meng Y and Hemley R J 2003 *Science* **302** 425
- [10] Patterson J R, Kudryavsev A and Vohra Y K 2002 *Appl. Phys. Lett.* **81** 2073
- [11] Fahy S, Louie S G and Cohen M L 1986 *Phys. Rev. B* **34** 1191
- [12] Yagi T, Utsumi W, Yamakata M, Kikegawa T and Shimomura O 1992 *Phys. Rev. B* **46** 6031
- [13] Furthmüller J, Hafner J and Kresse G 1994 *Phys. Rev. B* **50** 15606

- [14] Wang Z W, Zhao Y S, Tait K, Liao X Z, Schiferl D, Zha C S, Downs R T, Qian J, Zhu Y T and Shen T D 2004 *Proc. Natl Acad. Sci.* **101** 13699
- [15] Wang Z W, Zhao Y S, Zha C S, Xue Q, Downs R T, Duan R G, Caracas R Z and Liao X Z 2008 *Adv. Mater.* **20** 3303
- [16] MATERIAL STUDIOS 2005 *Version 4.0* Accelrys Software Inc.
- [17] Perdew J P and Wang Y 1992 *Phys. Rev. B* **45** 13244
- [18] Ceperley D M and Alder B J 1980 *Phys. Rev. Lett.* **45** 566
- [18] Perdew J P and Zunger A 1981 *Phys. Rev. B* **23** 5048
- [19] Vanderbilt D 1990 *Phys. Rev. B* **41** 7892
- [20] Monkhorst H J and Pack J D 1976 *Phys. Rev. B* **13** 5188
- [21] Pfrommer B G, Cote M, Louie S G and Cohen M L 1997 *J. Comput. Phys.* **131** 233
- [22] Sharma A K, Salunke H G, Das G P, Ayyub P and Multani M S 1996 *J. Phys.: Condens. Matter* **8** 5801
- [23] Raffy C, Furthmüller J and Bechstedt F 2002 *Phys. Rev. B* **66** 075201
- [24] Wen B, Zhao J J, Bucknum M J, Yao P K and Li T J 2008 *Diamond Relat. Mater.* **17** 356
- [25] Cline C F, Dunegan H L and Henderson G W 1967 *J. Appl. Phys.* **38** 1944
- [26] Gusev A A, Zehnder M M and Suter U W 1996 *Phys. Rev. Rep.* **54** 1
- [27] Nye J F 1964 *Physical Properties of Crystals* (Oxford: Clarendon)
- [28] Pugh S F 1954 *Phil. Mag.* **45** 823
- [29] Ravindran P, Fast L, Korzhavyi P A, Johansson B, Wills J and Eriksson O 1998 *J. Appl. Phys.* **84** 4891
- [30] Chu F, Lei M, Maloy S A, Petrovic J J and Mitchel T E 1996 *Acta Mater.* **44** 3035
- [31] Gao F M 2006 *Phys. Rev. B* **73** 132104
- [32] Bundy F P and Kasper J S 1967 *J. Chem. Phys.* **46** 3437
- [33] Brazhkin V V *et al* 2002 *Phil. Mag. A* **82** 231